

# We are IntechOpen, the world's leading publisher of Open Access books Built by scientists, for scientists

6,900

Open access books available

186,000

International authors and editors

200M

Downloads

Our authors are among the

154

Countries delivered to

TOP 1%

most cited scientists

12.2%

Contributors from top 500 universities



WEB OF SCIENCE™

Selection of our books indexed in the Book Citation Index  
in Web of Science™ Core Collection (BKCI)

Interested in publishing with us?  
Contact [book.department@intechopen.com](mailto:book.department@intechopen.com)

Numbers displayed above are based on latest data collected.  
For more information visit [www.intechopen.com](http://www.intechopen.com)



# Assisting Liquid Phase Sintering of Pure Aluminum (Al) by the Tin Addition

*Nur Ayuni Jamal, Farazila Yusof, Yusilawati Ahmad,  
Norhuda Hidayah Nordin and Suraya Sulaiman*

## Abstract

In the present study, the addition of tin (Sn) to the pure Al system was done, and its effects on the morphology, density, and compressive yield strength of pure Al were analyzed systematically. In this context, the morphology of sintered Al revealed enhanced wettability and sintering response between Al particles with increased Sn content. Moreover, physical characteristics of sintered Al alloys demonstrated oxidation phenomenon (black color specimen) with the lowest Sn content of 1.5 weight percent (wt.%), in which a higher Sn content of 2 and 2.5 wt.% produced silver color specimens, implying a reduction in oxidation. Additionally, densification of sintered Al alloys was greatly promoted with increased Sn contents, suggesting effective wetting as confirmed by the previous morphological observations. Similarly, the compressive yield strength of sintered Al alloys improved with increased Sn content which might be due to the enhanced inter-particle contacts between Al particles and sufficient wetting by molten Sn. Based on the results obtained, the introduction of Sn powder at various contents improved the sintering response of pure Al powder by providing sufficient liquid-phase sintering. Therefore, the sintered Al alloys had enhanced the morphological, densification, physical characteristics, and compressive yield strength.

**Keywords:** aluminum alloys, tin, liquid phase sintering, powder metallurgy, oxidation, sintered density, compressive strength

## 1. Introduction

Lightweight materials, especially aluminum (Al) and its alloys, are increasingly utilized in different industries because of their uniqueness, including high corrosion resistance, outstanding strength to weight ratio, excellent flexibility, thermal properties, and remarkable finishing properties [1–3]. As such, Al and its alloys are finding increased use in the fields of automotive, construction, marine, and aerospace. Solid-state and liquid-state processes are widely implemented to fabricate metals to obtain Al and its alloys that could be applied in the abovementioned fields [1, 4–7]. However, there is an increased interest in the solid-state process and practice due to its versatility, greater control of starting materials proportion, chemical

homogeneity, potential to fabricate near net shape with complex parts, and cost-effectivity [5–8]. The studies by Ji et al. [8] and Feijoo et al. [9] documented a noteworthy improvement in the ultimate tensile strength (UTS) of around 180 megapascals (MPa) and 377 MPa of an Al alloy system with an optimum reinforcement addition of 5 weight percent (wt.%) silicon carbide (SiC) and 0.5 wt.% multiwall carbon nanotubes, fabricated through powder metallurgy technique.

However, despite its advantages, the sintering of Al and its alloys is problematic due to a thermodynamically stable oxide layer on the particle surfaces. The scenario often hinders effective bond formations between the powder particles. Therefore, the accomplishment of desirable physical and mechanical performances could not be realized. Moreover, the presence of the unwanted oxide layer frequently promotes a nonwetting diffusion barrier for effective sintering of Al and its alloys [10–16]. Consequently, it is crucial to disrupt at least partially the oxide film, known as aluminum oxide ( $\text{Al}_2\text{O}_3$ ) or alumina, on the surfaces of Al particles. Therefore, the addition of sintering additives such as tin (Sn), zinc (Zn), and magnesium (Mg) to facilitate the liquid-phase sintering of Al and its alloys were introduced to minimize the issues [11–19]. Azadbeh and Razzaghi [15] reported that when 5.5 wt.% of Zn was introduced to an Al system, its densification and mechanical strength were improved at 119 HV and 564 MPa, respectively. Furthermore, a study performed by Liu et al. [16] documented that the addition of Sn (4 wt.%) could only provide sufficient liquid formation for effective liquid phase sintering of Al after the oxide layer on the Al surface has been interrupted via external load application or Mg addition. In this context, the authors recorded that the Al-Sn liquid development proceeded via melting of Sn followed by a repetition process of cracking and repairing owing to reoxidation and thermally induced stress of the exposed Al particles. Consequently, as the outer layer of Al particles scavenged the oxygen from the Argon (Ar) gas, the oxygen concentration in the core was reduced, accompanied by the creation of an Al-Sn liquid phase via the dissolution of the Al in the liquid Sn. Finally, sacrification of outer layers took place hence these layers remained porous. Additionally, the authors also suggested that an alternative mechanism by means of selection of irregular shape of Sn element could ensure maximum liquid formation during sintering of Al.

Therefore, the sintering of the Al cores proceeded through a typical liquid-phase sintering mechanism. Similarly, the utilization of sintering additives (Mg and Sn) enhanced the sintering response of sintered Al, which consequently improved its tensile strength up to 118 and 300 MPa, as discussed in the studies by Sercombe et al. [13] and MacAskill et al. [17]. Although there were extensive works on the sintering response of Al and its alloys fabricated via powder metallurgy technique, additional exploration is necessary, particularly with different formulations of Al and sintering additive. Consequently, the behavior of liquid-phase sintering of Al alloys was investigated in the current study by exploiting Sn constituent as sintering additive, developed through powder metallurgy technique. Moreover, Mg constituent at fixed content was also utilized in the current study to optimize the liquid phase formation by Sn constituent. Therefore, the reliability of the sintering response of Al alloys was systematically examined via its physical characteristics, oxygen content levels, compressive strength, density, and microstructure of the sintered Al alloys. The investigation aimed to provide an alternative solution to minimize the problematic sintering response of Al and its alloys.

## **2. Experimental procedure**

The base material, Al powder with 99.9% purity was purchased from NovaScientific (M) Sdn Bhd. The sintering additives to facilitate liquid phase

sintering of Al utilized elemental powders of Sn (99.5% purity) and Mg (99.9% purity) were supplied by NovaScientific (M) Sdn Bhd and Sigma Aldrich (M) Sdn Bhd, respectively. The information on the purity of these starting materials was provided by the respective suppliers. To observe the behavior of liquid phase sintering of Al alloys, varied content of Sn between 1.5, 2, and 2.5 wt.% and a constant 1 wt.% of Mg was added. Moreover, pure Al without the addition of Sn and Mg constituents was set as the reference material prior to study the effects of Sn and Mg in assisting liquid phase sintering of Al. As schematically illustrated in **Figure 1**, a powder metallurgy technique of mixing, compaction, and sintering was implemented to fabricate a sintered Al alloy. In this process, table-top ball milling was employed to prepare the elemental powder mixture comprised of Al, Sn, and Mg. The mixing was conducted for 2 h with the ball to powder ratio of 1 to 10, where zirconia balls were used as the ball milling medium to produce a homogenous elemental powder mixture. Consequently, the elemental powder mixture was pressed into cylindrical pellets of 10 mm diameter and 6 mm height under a constantly applied pressure of 250 MPa. Then, the compacted specimens were sintered under a protected environment of argon (Ar) gas at 580°C for 2 h to obtain pure sintered Al alloys. The sintered alloys were then cleaned with acetone to remove impurities, followed by drying in an oven for 12 h to prepare them for characterization. The microstructure of as received starting materials and elemental powder mixture were analyzed under scanning electron microscopy (SEM) (SEM, Jeol JSM6500F, JEOL Ltd., Tokyo, Japan) before they were employed to fabricate the sintered Al alloy. The step was essential to develop satisfactory sintered Al alloys

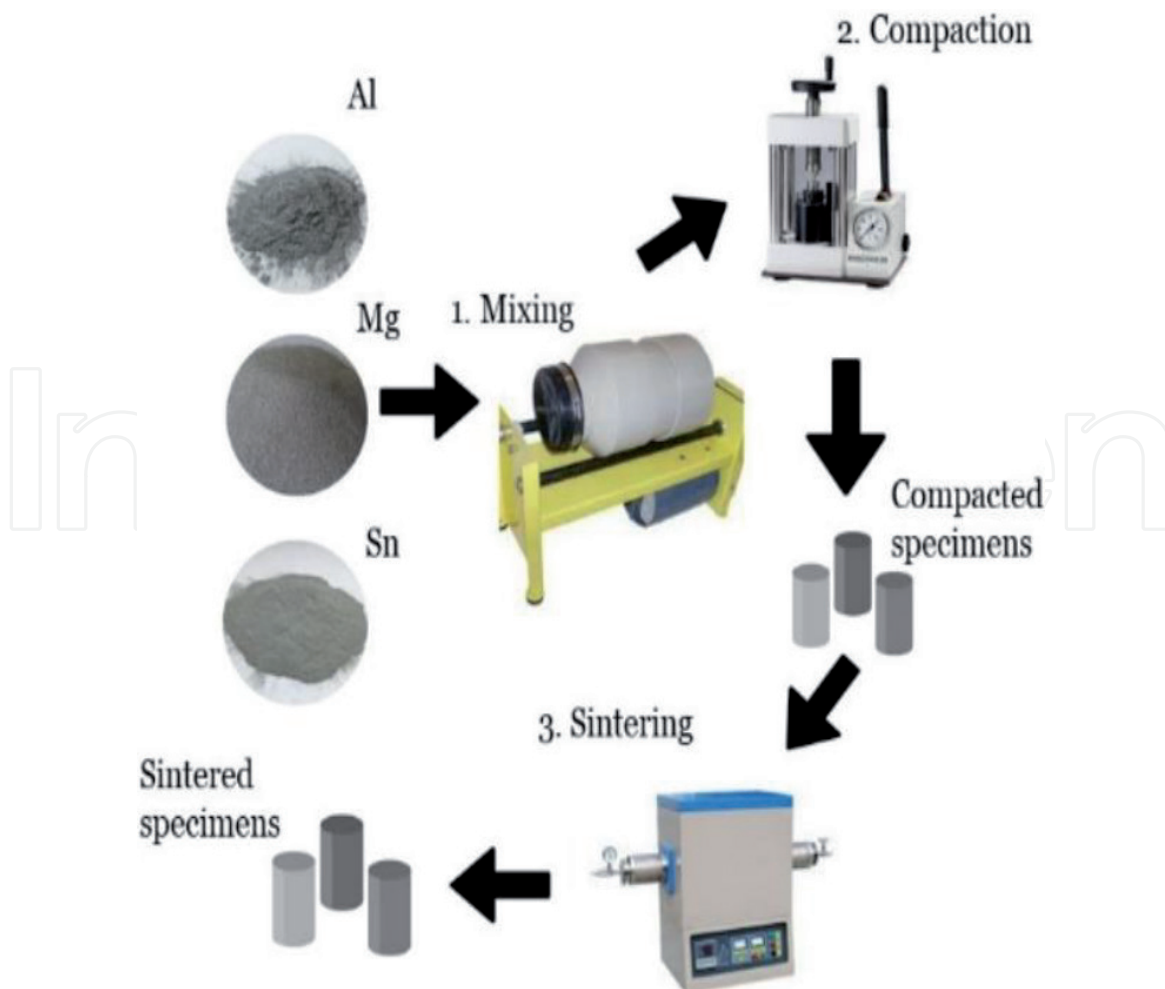


**Figure 1.**  
*Schematic diagram of the development of Al alloys by powder metallurgy technique.*

with desirable performance. A cross-section of sintered Al alloys was prepared for microstructure observation through SEM. Collectively, the residual oxygen content of the Al alloys at every stage was monitored by energy dispersive spectroscopy (EDS). Furthermore, any possibility of phase changes of the elemental powder mixture and the sintered Al alloys were identified using x-ray diffraction (XRD) analysis (XRD; PANalytical empyrean 1032, Eindhoven, Netherlands) in the  $2\theta$  range of  $20\text{--}80^\circ$ . Moreover, the step size of  $0.05$  degrees, radiation source of Cu  $K\alpha$  and accelerating voltage and current of  $40$  kV and  $40$  mA were also set for the XRD test conditions. Finally, the sintered density of the resultant Al alloys was determined via the Archimedes principle, as per ASTM C830-93. Similar experimental procedure was performed in fabricating the reference material (pure Al).

### 3. Results and discussion

#### 3.1 Microstructure of the starting materials and elemental powder mixture

The microstructure of the starting materials and elemental powder mixture is illustrated in **Figure 2(a–c)** and **Figure 3(a–c)**. From the observations, most of the Al and Mg particles were spherical, with some irregularities observed on the Al particles. These particles were calculated to have an average particle size of  $45$  and  $10$   $\mu\text{m}$ , respectively. On the contrary, the shape of the Sn particles was found to be mainly irregular with an average particle size of  $45$   $\mu\text{m}$ , as revealed in **Figure 2(c)**. Since the sintering of Al powder prevented the solid-state sintering process, it was crucial to disrupt the stable

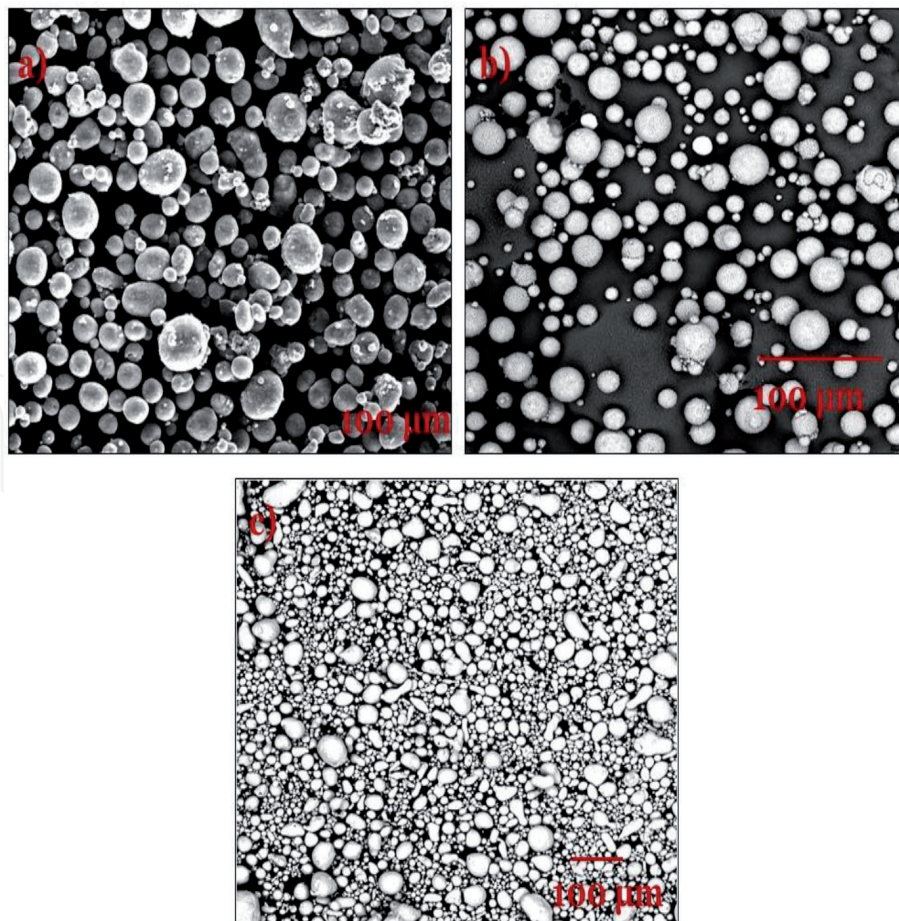


**Figure 2.** Microstructure of the starting materials of (a) Al powder, (b) Mg powder, and (c) Sn powder as observed under SEM.

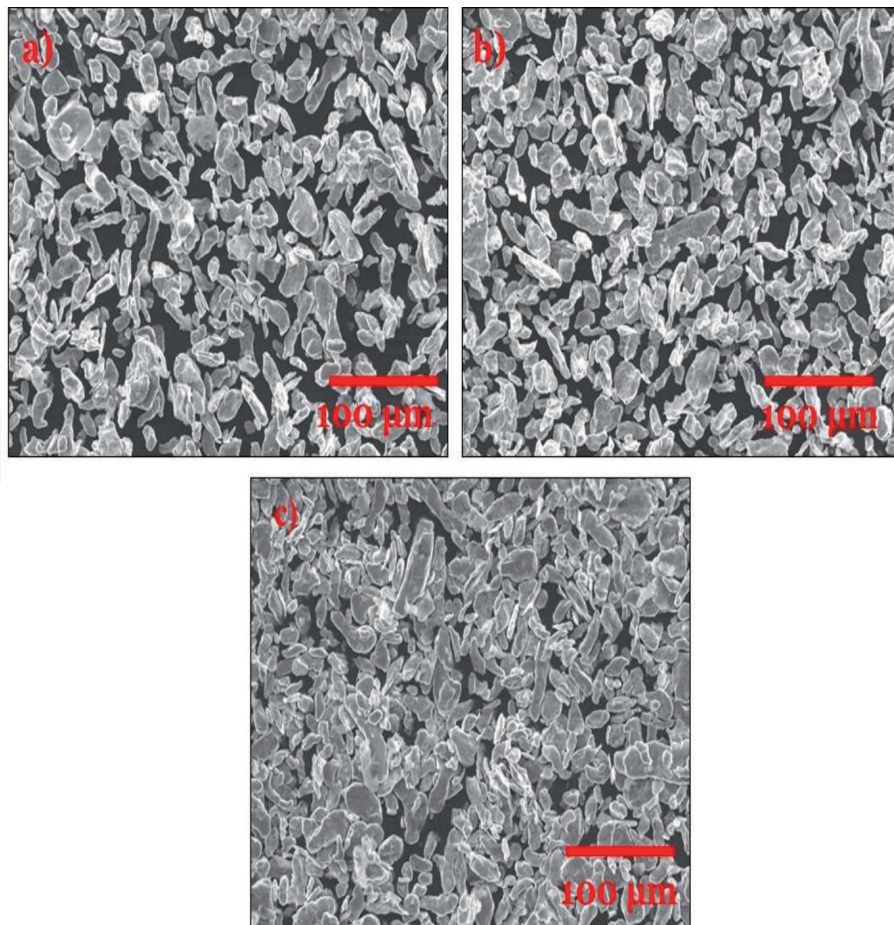


**Figure 3.** Microstructure of elemental powder mixture at different Sn content of (a) 1.5 wt.%, (b) 2 wt.%, and (c) 2.5 wt.% as observed under SEM.

oxide film that readily existed on the surface of the Al particles so that strong metallurgical bonds between the particles could be guaranteed. Therefore, the current investigation employed liquid phase sintering of Al alloys with Sn as the sintering additive. Sn was introduced to promote the liquid phase of Al because of its low melting temperature (232°C) compared to Al (660°C). However, the process could only be successful in the presence of Mg. The addition of Mg was reported to reduce the surface oxide of Al by exposing the underlying metal thus resulting in possible wetting of the Al particles by liquid Sn [14, 18–19]. On the other hand, the absence of powder mixture accumulation and homogenous distribution were identified after 12 h of mixing, suggesting optimal mixing condition in preparing elemental powder mixture of Al, Sn, and Mg, as demonstrated in **Figure 2(d)**. Regardless of different Sn content, the resultant particles of the elemental powder mixture were found to exhibit a lamellar structure, as evidenced in **Figure 3(a–c)**, respectively. These Sn particles were also identified to be flattened and elongated, having an average particle size of 50 μm. The resultant microstructure of the elemental powder mixture could be due to the repeated welding, fracturing, and rewelding of the elemental powder particles during mixing via ball milling technique [20]. Nevertheless, the overlapping and intimate contact between Sn particles were also clearly visible with increasing Sn content, confirming an increased Sn content in the elemental powder mixture, as seen in **Figure 3(a–c)**, respectively.

### 3.2 Visual inspection of the sintered aluminum alloys

The visual inspection of the sintered Al alloys at various Sn contents are depicted in **Figure 4(a–c)**. It was observed that the addition of 1.5 wt.% of Sn

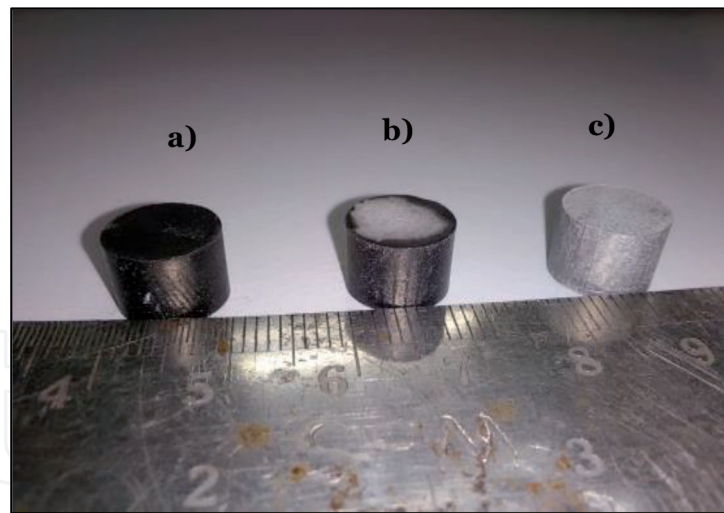


**Figure 4.** Visual inspection of the resultant Al alloys with different Sn content of (a) 1.5 wt.%, (b) 2 wt.%, and (c) 2.5 wt.%.

(the lowest amount) produced a black-colored Al alloy after sintering, implying oxidation and the ineffective role of Sn in increasing the fluidity of the Al alloy during sintering. However, when the Sn content was increased to 2 wt.%, the black-colored Al alloy changed slightly to silver that appeared only at the top of the alloy, suggesting insufficient liquid formation to enhance the Al alloy fluidity that consequently minimizing oxidation. Similar observation was also reported in the study of Pan et al. [21]. On contrary, the effects were more pronounced when the Sn content was maximized to 2.5 wt.% as the color of Al alloys completely replicated the original silver color of the Al powder, confirming complete interruption of the stable oxide film on the surfaces of Al during sintering. Furthermore, the findings were supported by the results obtained from the oxygen content analysis as tabulated in **Table 1**. A significantly decreased oxygen content of the resultant Al alloys from 0.58 to 0.44 wt.% was recorded when the content of Sn was increased from 1.5 to 2.5 wt.%, respectively. The results showed that the amount of Sn influenced the oxygen content of the resultant Al alloys. Therefore, as the Sn content was increased in the Al alloys, the oxygen level decreased, indicating an improvement of the overall wetting characteristics of the Al alloys. However, the addition of Mg constituent was also essential in assisting the formation of Sn liquid by reducing the oxide layer on the Al surface [4, 18–19]. According to Kondoh et al. [14], Mg addition was found to assist the distribution of Sn liquid below the oxide layer, thus contributing to successful wetting of Al by Sn liquid.

### 3.3 Microstructure of the resultant aluminum alloys

The cross-section of the sintered Al alloys at 1.5, 2, and 2.5 wt.% of Sn are demonstrated in **Figure 5(a–c)**, respectively. Moreover, the cross section of the pure Al without Sn and Mg addition (reference sample) is shown in **Figure 5(d)**. Based on the observations, the reference sample exhibited poor sintering response; evidenced by visible appearance of individual particles as if no sintering process has been performed. Furthermore, the presence of large number of pores between the individual particles were obvious, confirming ineffective sintering of pure Al. Similarly, pores or inter-particle voids between the grain boundaries were also noticeable when the Sn amount in the Al system was the lowest (1.5 wt.%), portraying a poor sintering response. However, the microstructure of 1.5 wt.% containing Al was slightly improved in comparison to pure Al without Sn addition.

Tin content (wt.%)	Oxygen content (wt.%)
Elemental powder mixture	0.22 ± 0.10
1.5 (sintered at 580°C)	0.58 ± 0.12
2 (sintered at 580°C)	0.51 ± 0.13
2.5 (sintered at 580°C)	0.44 ± 0.11

**Table 1.**

Oxygen content reading of elemental powder mixture and sintered Al alloys at various Sn content from EDS analysis. Data are presented in mean ± standard deviation.

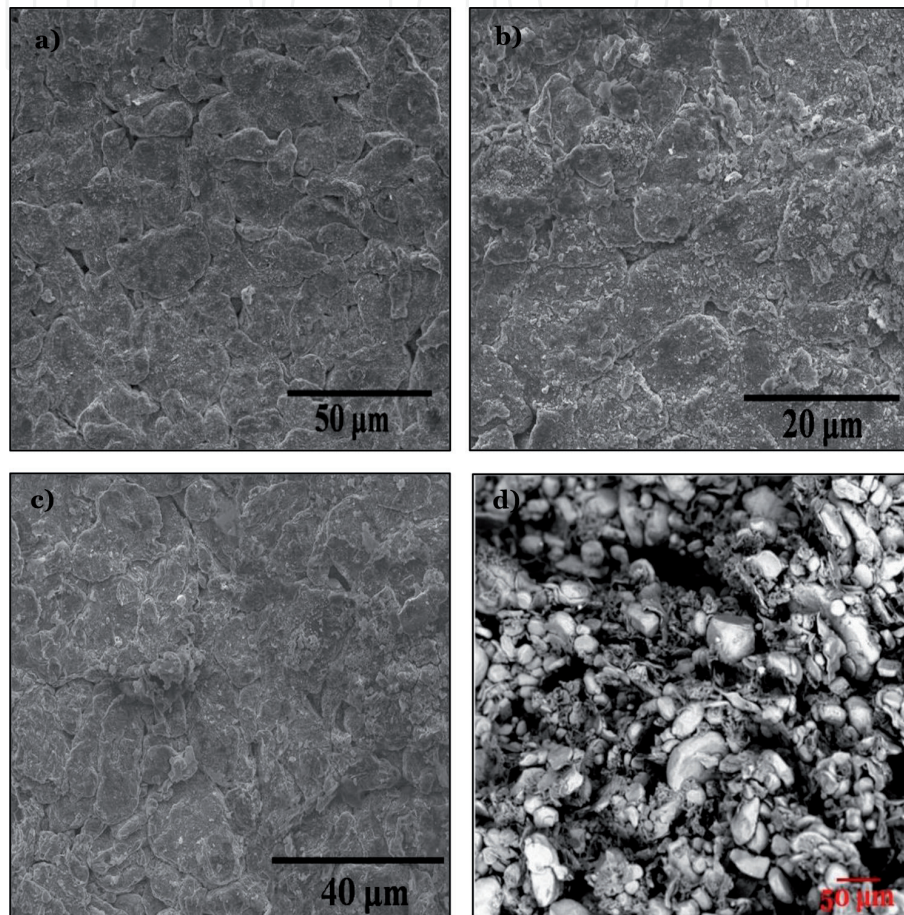


**Figure 5.**

Microstructures of the resultant Al alloys at various Sn content of (a) 1.5 wt.%, (b) 2 wt.%, (c) 2.5 wt.%, and (d) pure Al without Sn and Mg constituents (reference sample).

Therefore, the results might be associated with insufficient pore rounding as evidenced by the appearance of elongated pores, an abundance of grain boundaries, and negligible inter-particle necking [17–19, 22]. Moreover, the addition of Sn might be inadequate to occupy both the elongated and rounded pores, preventing a more favorable packing grains arrangement that could bring the solid particles closer, which contributed to grain growth and densification failure. On the contrary, improved sintering response was observed with increased Sn content, particularly at 2 and 2.5 wt.%, owing to the increased presence of pores rounding and lesser particle boundaries. Additionally, grain growth development was observed with increased Sn content as the amount of liquid formation was sufficient to fill the existing pores that successfully brought the solid particles together, improving the sintering quality of the resultant Al specimens. According to Aneta [23], a desirable liquid phase enhanced mass transport, which encouraged the rearrangement and fragmentation of solid particles. The phenomenon was especially true as

the formation of inter-particle necking became increasingly visible with increased pore rounding, as shown in **Figure 5(b and c)**.

Furthermore, successful wetting of Sn elements on the surfaces of the Al particles enhanced the metallurgical bonds between the Al particles, attributable to higher and sufficient liquid phase formation that filled the remaining pores in the Al system [17–19, 22, 24]. Therefore, the addition of higher Sn content produced a permanent liquid phase that improved the densification and sintering quality of the alloys (mainly for Al added with 2 and 2.5 wt.% of Sn). Undetectable clustering of Sn particles represented by the bright phases indicated a uniform distribution of Sn particles along the grain boundaries of the Al alloys, especially with the addition of 2 and 2.5 wt.% of Sn that further promoted effective liquid phase formation. Consequently, densification and compressive strength of the Al alloys were elevated, as evidenced in **Figures 6 and 7**, respectively. According to MacAskill et al. [17], such morphologies confirmed the liquid formation by molten Sn during sintering that was capable of wetting the surface of Al and scattered evenly

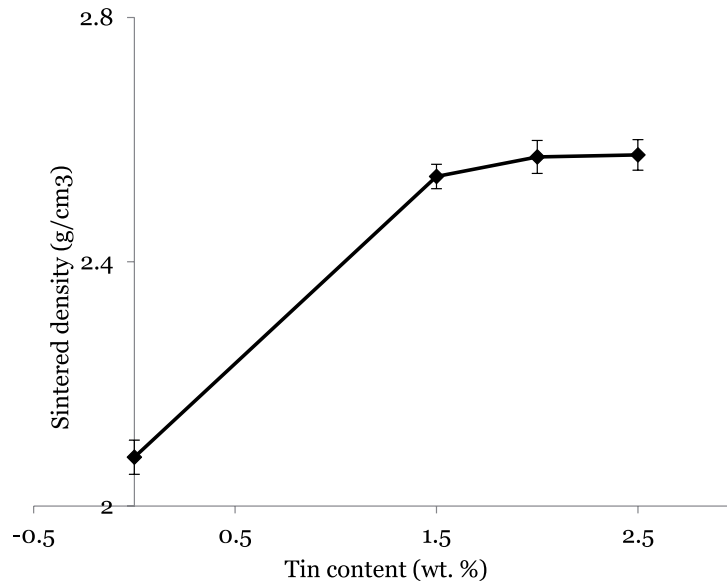


**Figure 6.**  
The effect of Sn variation on the sintered densities of the resultant Al alloys.

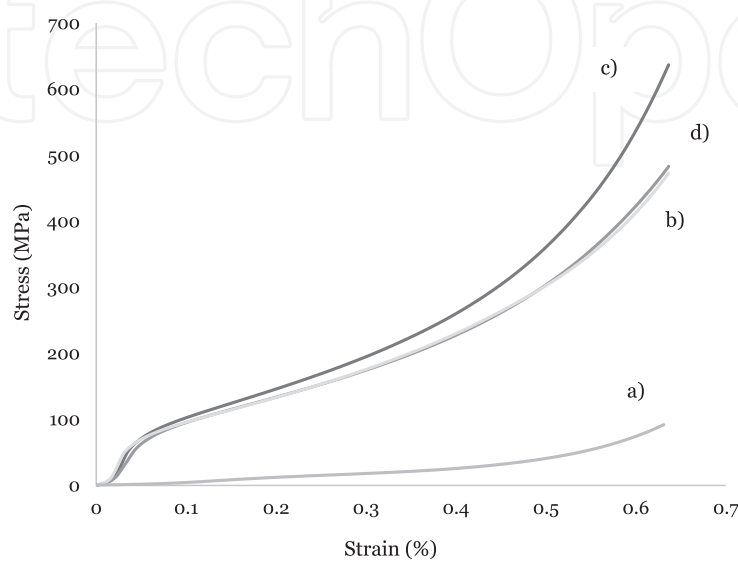


**Figure 7.**  
Stress-strain curve of resultant (a) pure Al and Al alloys with different Sn content of (b) 1.5 wt.%, (c) 2 wt.%, and (d) 2.5 wt.%.

throughout the Al alloys. However, the occurrence could only be accomplished by the existence of Mg due to its potential to stimulate the wetting response of molten Sn. However, higher Sn content of up to 2.5 wt.% slightly reintroduced several particle boundaries as shown in **Figure 4(c)**. The observation might be due to the remaining unreacted Sn that was unable to wet the Al surfaces, which hindered effective liquid phase formation during sintering [25]. Moreover, Sercombe et al. [13] reported a similar observation.

### 3.4 Phases transformation of the resultant aluminum alloys

The X-ray diffraction (XRD) patterns of pure Al without Sn and Mg addition as well Al alloys at different Sn content (1.5, 2, and 2.5 wt.%) are presented in **Figure 8(a–d)**. The dominant XRD phases of the resultant Al alloys were mainly attributed to the  $\alpha$ -Al constituent, characterized by the (111), (200), (220), and (311) diffraction peaks at 38.87, 45.42, 67.16, and 78.54°, respectively. As can be seen in **Figure 8(a)**, the peak intensities of pure Al were found to be lower compared to the 1.5, 2, and 2.5 wt.% Sn containing Al alloys. This is probably due to poor sintering response in the absence of Sn and Mg constituents hence low crystalline formation during complete sintering. In the case of Al alloys, the peak intensities of Sn increased with increased Sn content, confirming the addition of Sn during the process. The absence of the Mg peak in the Al system was attributed to the dissolution of Mg in  $\alpha$ -Al [17, 26]. Based on the Al-Mg binary equilibrium phase diagram, Mg addition up to maximum content of 18.6% could be completely dissolved in the parent Al phase at the eutectic temperature of 450°C [27]. Moreover, it has been

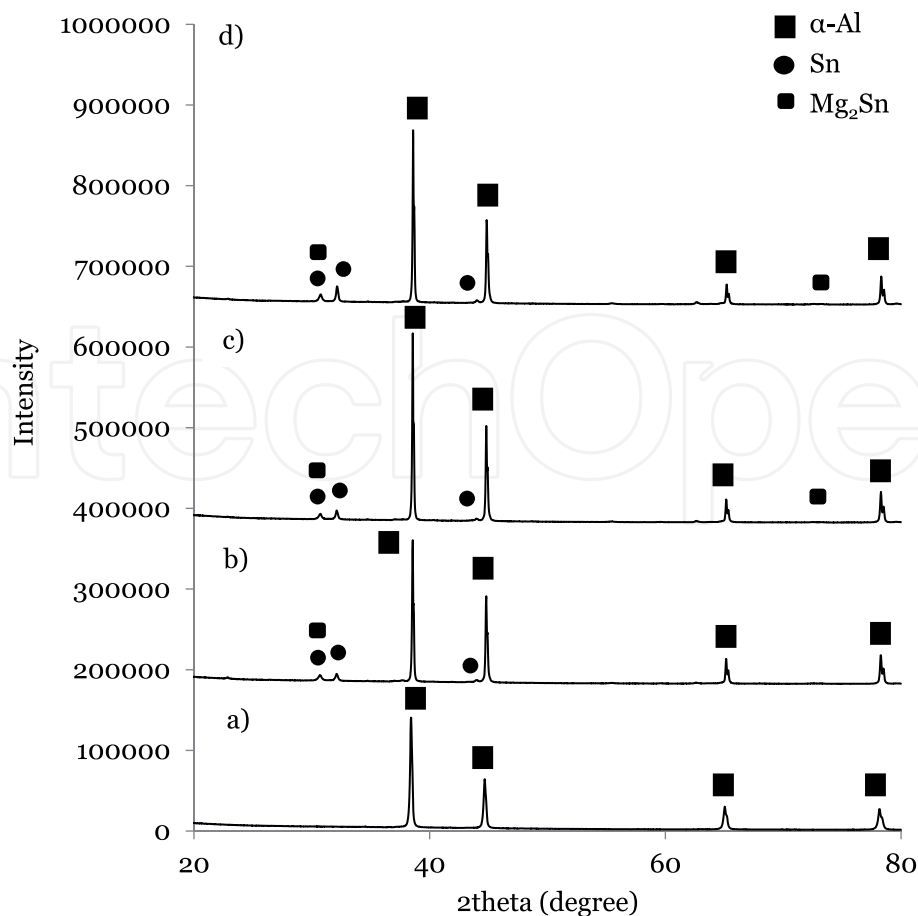


**Figure 8.** Phases transformation of (a) Pure Al and Al alloys with different Sn content of (b) 1.5 wt.%, (c) 2 wt.%, and (d) 2.5 wt.%.

reported that the creation of brittle intermetallic compounds ( $\beta$ -Al<sub>3</sub>Mg<sub>2</sub> phase) that has associated with poor mechanical performance was observable with increasing Mg content [28]. For this reason, its utilization should be maximized up to 5 and 10 wt.% for wrought alloys and cast alloys, respectively [28]. Moreover, it was documented that Mg vaporized during sintering, and the gas produced served as a reliable gettering agent for effective liquid phase sintering of Al [14, 26, 29–30]. Therefore, it has been proposed that the application of nitrogen (Ni) as a sintering atmosphere was effective in transporting Mg vapor (effective gettering agent) around the pore network via the formation of magnesium nitride (Mg<sub>3</sub>N<sub>2</sub>) [29]. On the contrary, Schaffer and Hall [29] documented that Mg could be effectively transported as a vapor in Ar atmosphere which is comparable to the Ni atmosphere considering higher vapor pressure of Mg as compared to Mg<sub>3</sub>N<sub>2</sub> formation. On the other hand, weak peaks of Mg<sub>2</sub>Sn compounds were observed in the current study with a higher Sn amount (2 and 2.5 wt.%), postulating solidification of the Mg<sub>2</sub>Sn compounds within the Al phase [31]. This is essential for optimum attainment of physical and mechanical performance of the resultant alloys [31]. It is important to note that a lower sintering temperature of 580°C that was set in the current study prevented the formation of higher peaks of the Mg<sub>2</sub>Sn compounds. Therefore, future studies should analyze the effects of various sintering temperatures other than the current setting on the sintering response of Al alloys.

### 3.5 Sintered densities of the resultant aluminum alloys

**Figure 6** presents the sintered densities of pure Al and 1.5, 2, and 2.5 wt.% Sn containing Al alloys. Based on the findings, the densification of pure Al was found to enhance from 2.083 g/cm<sup>3</sup> to 2.5397 g/cm<sup>3</sup>, 2.573 g/cm<sup>3</sup> and 2.575 g/cm<sup>3</sup>, with the addition of Sn content from 1.5 to 2 wt. % and 2.5 wt.%, respectively. A comparable observation was documented in previous literature [23–24, 26, 30]. The low sintered density value of pure Al might be due to the noticeable appearance of individual particles and large number of pores formation hence portraying poor sintering response as evidenced in **Figure 5(d)**. In contrast, the addition of a higher amount of Sn reduced micro pores formation and diminished particle boundaries, which improved the sintered densities as shown in **Figure 5(b–d)**. Moreover, the lessened appearance of elongated pores might have promoted the densification effects in the current study. According to Ozay et al. [24], enhanced densification might be the result of filled gaps between the powder particles through the action of molten Sn, which also contributed to reduced porosity. Furthermore, Sercombe et al. [13] suggested that improved wetting effects with the implementation of higher Sn content led to reduced surface tension as Sn dispersed into the liquid phase during sintering. Atabay et al. [31] also highlighted that the existence of Mg<sub>2</sub>Sn intermetallic compounds contributed to the positive effects of densification of the Al alloys. Therefore, the highest sintered density of the Al alloys was observed when 2.5 wt.% of Sn was added. This is further supported by the higher and more intense visible XRD peaks of the intermetallic compounds compared to the pure Al and Al alloys with 1.5 wt.% of Sn as demonstrated in **Figure 7(c)**.

### 3.6 Compressive strength of resultant aluminum alloys

A compressive test was conducted to evaluate the response of the pure Al and 1.5, 2, and 2.5 wt.% Sn containing Al alloys under a compressive load. The stress-strain curve of the resultant pure Al and Al alloys with varying Sn content is shown in **Figure 7**. The obtained stress-strain curve of the pure Al and Al alloys

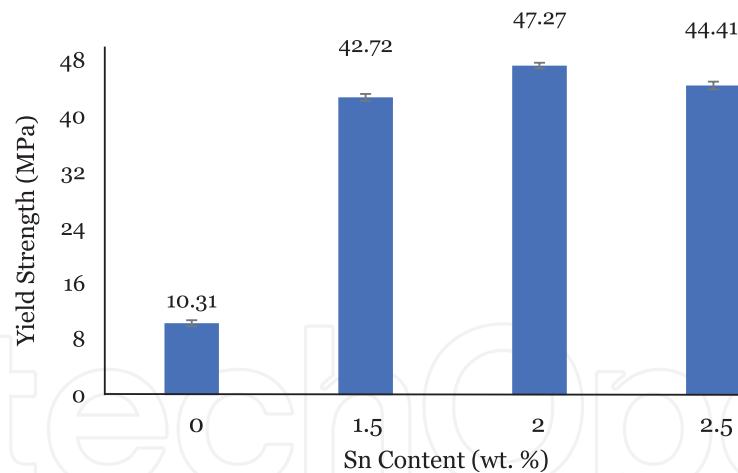


**Figure 9.**  
*Compressive yield strength of pure Al and Al alloys with different Sn content of 1.5, 2, and 2.5 wt.%.*

obeyed the typical stress-strain curve of Al and its alloys. To better understand, the compressive yield strength of the pure Al and Al alloys is displayed in **Figure 9**. Based on the findings, the compressive yield strength of the pure Al demonstrated the lowest yield strength value of 10.31 MPa, implying poor sintering response owing to the presence of individual particles with greater number of pores formation as seen in **Figure 5(d)**. This shows that the absence of Sn as sintering additive in combination with Mg constituent was unfavorable in promoting the liquid phase sintering of pure Al. On the other hand, Al alloys exhibited an increasing trend from 42.72 to 47.27 MPa with the Sn content of 1.5 and 2 wt.%, respectively. However, the addition of 2.5 wt.% Sn (the highest) reduced the compressive yield strength of the Al alloys from 47.27 (2 wt.% Sn) to 44.21 MPa. Therefore, the results were inconsistent with the results from the sintered density measurements, presumably due to a slightly increased particle boundary or grain coarsening, as revealed in **Figure 5(c)**. Furthermore, parallel observations were also discussed by Padmavathi and Upadhyaya [26].

Although the presence of Mg<sub>2</sub>Sn compounds (**Figure 8(b and c)**) produced substantial improvements in the mechanical performance of Al and its alloys, the effects of grain coarsening were more pronounced, which reduced the compressive yield strength of the Al alloys when the Sn content was maximized to 2.5 wt.% [31]. Moreover, it was reported that excessive content of Sn caused undiffused liquid phase to remain at the particle boundary and led to the brittle creation of particle boundary networks, that consequently reduced the mechanical performance of Al and its alloys [13, 31, 17–19]. Therefore, it could be hypothesized that particle boundary enlargement and liquid phase profusion might contribute to the decreased compressive strength of the Al alloys that were fabricated in the current study.

#### 4. Conclusion

The utilization of Sn element that served as sintering additive in the current study significantly improved the sintering response of the resultant Al alloys that were fabricated via powder metallurgy technique. The varying Sn content between 1.5, 2, and 2.5 wt.% enhanced the properties of the resultant Al alloys in terms of their physical appearance, from black to silver-like coloring due to oxidation-reduction, and sintered densities from 2.5397 to 2.575 g/cm<sup>3</sup> as the gaps between particles were filled by molten Sn, which lessened pore formation and appearance of particle

boundary. Therefore, the microstructure of the resultant Al alloys confirmed the pore rounding and diminished particle boundary that led to the improved metallurgical bonding between the Al particles.

Additionally, the compressive yield strength of the resultant Al alloys increased from 42.72 to 47.27 MPa with an increased amount of Sn (from 1.5 to 2 wt.%), which were the result of diminished particle boundary and reduced pores formation. However, despite a positive increment in the sintered density of the Al alloys with increased Sn content of up to 2.5 wt.%, the compressive yield strength was slightly reduced. The finding might be attributed to the excessive liquid phase formed along with the visible appearance of particle boundary or grain coarsening. In conclusion, the study showed that the addition of Sn as sintering additive successfully promoted the Al alloys liquid phase sintering, especially with increased Sn content.

## **Acknowledgements**

The authors would like to express sincere gratitude to the International Islamic University Malaysia (IIUM) and the Ministry of Higher Education (MOHE) Malaysia for sponsoring the current project under the grant number of FRGS/1/2019/TK08/UIAM/02/5.

## **Author details**

Nur Ayuni Jamal<sup>1\*</sup>, Farazila Yusof<sup>2</sup>, Yusilawati Ahmad<sup>3</sup>, Norhuda Hidayah Nordin<sup>1</sup> and Suraya Sulaiman<sup>4</sup>

1 Manufacturing and Materials Engineering (MME) Department, Kulliyyah of Engineering, International Islamic University Malaysia (IIUM), Kuala Lumpur, Malaysia

2 Centre of Advanced Manufacturing and Material Processing (AMMP Centre), Universiti of Malaya, Kuala Lumpur, Malaysia

3 Biotechnology Engineering Department, Kulliyyah of Engineering, International Islamic University Malaysia (IIUM), Kuala Lumpur, Malaysia

4 Fakulti Teknologi Kejuruteraan Pembuatan dan Mekatronik, Universiti Malaysia Pahang (UMP), Pekan, Pahang, Malaysia

\*Address all correspondence to: ayuni\_jamal@iium.edu.my

## **IntechOpen**

© 2021 The Author(s). Licensee IntechOpen. This chapter is distributed under the terms of the Creative Commons Attribution License (<http://creativecommons.org/licenses/by/3.0>), which permits unrestricted use, distribution, and reproduction in any medium, provided the original work is properly cited. 

## References

- [1] Emamy M, Pourbahari B, Malekan M. Effects of Mg<sub>2</sub>Sn intermetallic on the microstructure and tensile properties of Al-15% Mg<sub>2</sub>Si-X% Sn composite. *Journal of Materials Research*. 2016;**31**(24):1-9. DOI: 10.1557/jmr.2016.426
- [2] Banerjee S, Robi PS, Srinivasan A, Lakavath PK. Effect of trace additions of Sn on microstructure and mechanical properties of Al-Cu-Mg alloys. *Materials and Design*. 2010;**31**(8):4007-4015. DOI: 10.1016/j.matdes.2010.03.012
- [3] Aliyu IK, Saheb N, Hassan SF, Al-Aqeeli N. Microstructure and properties of spark plasma sintered aluminum containing 1 wt.% SiC nanoparticles. *Metals*. 2015;**5**(1):70-83. DOI: 10.3390/met5010070
- [4] Boland CD, Bishop D, Donaldson I, Hexemer Jr RL. On the development of an aluminum P/M Alloy for “Press-Sinter-Size” Technology. In: *Proceedings of the International Conference on Powder Metallurgy & Particulate Materials (PowderMet 2010)*; 27-30 June 2010; Princeton: The Metal Powder Industries Federation (MPIF); 2010. pp. 1-14
- [5] Qiu F, Gao X, Tang J, Gao YY, Shu SL, Han X, et al. Microstructures and tensile properties of Al-Cu matrix composites reinforced with nano-sized SiCp fabricated by semisolid stirring process. *Metals*. 2017;**7**(2):1-8
- [6] Mahesh L, Reddy JS. Development and characterization of titanium nitride reinforced aluminium MMC's through powder metallurgy technique. *Mechanics and Mechanical Engineering*. 2017;**21**(1):29-36
- [7] Ervina Efzan MN, Siti Syazwani N, Mohd Mustafa ABA. Fabrication method of aluminum matrix composite (AMCS): A review. *Key Engineering Materials*. 2016;**700**:102-110. DOI: 10.4028/www.scientific.net/KEM.700.102
- [8] Ji X, Zhang C, Li S. In situ synthesis of core-shell-structured SiCp reinforcements in aluminium matrix composites by powder metallurgy. *Metals*. 2021;**11**(8):1-15. DOI: 10.3390/met11081201
- [9] Feijoo I, Pena G, Cabeza M, Cristobal MJ, Rey P. MWCNT-reinforced AA7075 composites: Effect of reinforcement percentage on mechanical properties. *Metals*. 2021;**11**(6):1-19. DOI: 10.3390/met11060969
- [10] Dolgoplov NA, Petelin AL, Rakov SV, Simanov AV. Penetration of liquid tin along grain boundaries and triple grain-boundary junctions of aluminum. *Russian Journal of Non-Ferrous Metals*. 2007;**48**(2):126-130. DOI: 10.3103/S1067821207020101
- [11] Du X, Liu R, Xiong X, Liu H. Effects of sintering time on the microstructure and properties of an Al-Cu-Mg alloy. *Journal of Materials Research and Technology*. 2020;**9**(5):9657-9666. DOI: 10.1016/j.jmrt.2020.06.083
- [12] Momeni H, Razavi H, Shabestari SG. Effect of supersolidus liquid phase sintering on the microstructure and densification of the Al-Cu-Mg pre-alloyed powder. *Iranian Journal of Materials Science and Engineering*. 2011;**8**(2):10-17
- [13] Sercombe TB, Schaffer GB. On the use of trace additions of Sn to enhance sintered 2xxx series Al powder alloys. *Materials Science and Engineering A*. 1999;**68**(1-2):32-39. DOI: 10.1016/S0921-5093(99)00126-4
- [14] Kondoh K, Kimura A, Takeda Y, Watanabe R. Behavior of magnesium

and tin at the surface of aluminum-silicon-magnesium-tin alloy powder particles at elevated temperature and their effect on direct nitriding reaction. *Journal of the Japan Institute of Metals*. 2000;**64**(11):1106-1112

[15] Azadbeh M, Razzaghi ZA. Properties evolution during transient liquid phase sintering of PM alumix 431. *Advances in Materials Science and Engineering*. 2009;**2009**(648906):1-5. DOI: 10.1155/2009/648906

[16] Liu ZY, Sercombe TB, Schaffer GB. The effect of particle shape on the sintering of aluminum. *Metallurgical and Materials Transactions A*. 2007;**38**:1351-1357. DOI: 10.1007/s11661-007-9153-2

[17] MacAskill IA, Hexemer RL Jr, Donaldson IW, Bishop DP. Effects of magnesium, tin and nitrogen on the sintering response of aluminum powder. *Journal of Materials Processing Technology*. 2010;**210**(15):2252-2260. DOI: 10.1016/j.jmatprotec.2010.08.018

[18] Schaffer GB, Huo SH, Drennan J, Auchterlonie GJ. The effect of trace elements on the sintering of an Al-Zn-Mg-Cu alloy. *Acta Materilia*. 2001;**49**(14):2671-2678. DOI: 10.1016/S1359-6454(01)00177-X

[19] Schaffer GB, Sercombe TB, Lumley RN. Liquid phase sintering of aluminium alloys. *Materials Chemistry and Physics*. 2001;**67**(1-3):85-91. DOI: 10.1016/S0254-0584(00)00424-7

[20] Suryanarayana C. Mechanical alloying and milling. *Progress in Materials Science*. 2001;**46**:1-184. DOI: 10.1016/S0079-6425(99)00010-9

[21] Pan Y, Lua X, Hayat MD, Yang F, Liu CC, Li Y, et al. Effect of Sn addition on the high-temperature oxidation behavior of high Nb containing TiAl alloys. *Corrosion Science*. 2020;**166**(108449):1-11. DOI: 10.1016/j.corsci.2020.108449

[22] Schaffer GB, Yao JY, Bonner SJ, Crossin E, Pas SJ, Hill AJ. The effect of tin and nitrogen on liquid phase sintering of Al-Cu-Mg-Si alloys. *Acta Materilia*. 2008;**56**(11):2615-2624. DOI: 10.1016/j.actamat.2008.01.047

[23] Aneta SN. The effect of the addition of boron on the densification, microstructure and properties of sintered 17-4 Ph stainless steel. *Technical Transactions: Mechanics*. 2014;**111**(2-M):85-96

[24] Ozay C, Gencer EB, Gokce A. Microstructural properties of sintered Al-Cu-Mg-Sn alloys. *Journal of Thermal Analysis and Calorimetry*. 2018;**134**:23-33. DOI: 10.1007/s10973-018-7171-5

[25] Gu ML, Zhang JH, Wei Z. Effect of sintering aid on microstructure and mechanical properties of TiB<sub>2</sub>/Tin tool materials. *Advanced Materials Research*. 2011;**287-290**:1933-1937. DOI: 10.4028/www.scientific.net/AMR.287-290.1933

[26] Padmavathi C, Upadhyaya A. Sintering behavior and mechanical properties of Al-Cu-Mg-Si-Sn aluminum alloy. *Transactions of the Indian Institute of Metals*. 2011;**64**:345-357. DOI: 10.1007/s12666-011-0089-2

[27] Massalski TB. Binary alloy phase diagrams. In: Okamoto H, Subramanian PR, Kacprzak L, editors. *Advanced Materials*. Ohio, USA: ASM International, Materials Park; 1991. p. 3589. DOI: 10.1002/adma.19910031215

[28] Harada Y, Jiang N, Kumai S. Mechanical properties of cold-rolled and annealed Al-12%Mg alloy sheet with high Mg solid solubility fabricated from vertical-type high-speed twin-roll cast strip. *Materials Transactions*. 2019;**60**(11):2435-2441. DOI: 10.2320/matertrans.f-m2019850

[29] Schaffer GB, Hall BJ. The influence of the atmosphere on the sintering of

aluminum. Metallurgical and Materials  
Transactions A. 2002;**33**(10):3279-3284.  
DOI: 10.1007/s11661-002-0314-z

[30] Dudas JH, Thompson CB. Improved  
sintering procedures for aluminum P/M  
parts. In: Hausner HH, editor. Modern  
Developments in Powder Metallurgy.  
Boston, MA: Springer; 1971. p. 490.  
DOI: 10.1007/978-1-4615-8963-1\_2

[31] Atabay SE, Esen Z, Dericioglu AF.  
Effect of Sn alloying on the diffusion  
bonding behavior of Al-Mg-Si alloys.  
Metallurgical and Materials  
Transactions A. 2017;**48**:3181-3187. DOI:  
10.1007/s11661-017-4089-7

IntechOpen